A Coupled Interaction Model for Simulation and Mitigation of Interdependent Cascading Outages

Leibao Wang, Junjian Qi, *Senior Member, IEEE,* Bo Hu, *Member, IEEE,* and Kaigui Xie, *Senior Member, IEEE*

***Abstract*—In this paper, a coupled interaction matrix is proposed to describe the interactions between line outages and the load shed at buses. The coupled interaction matrix is effectively estimated by the Expectation Maximization algorithm. A highly probabilistic coupled interaction model is further proposed to efficiently generate cascades with both line outages and the load shed based on the coupled interaction matrix and the distribution of initial outages. To mitigate cascading failures, critical links are identified based on the coupled interaction matrix by calculating a comprehensive severity index that considers the consequences of both line outages and the load shed. Simulation results on the IEEE 300-bus system verify the effectiveness of the proposed approach. The cascades generated from the coupled interaction model match the statistics of the original cascades very well. The identified critical links based on the comprehensive severity index enable a proper tradeoff between reducing line outages and reducing the load shed, leading to a better mitigation effect than only considering either line outages or the load shed.**

***Index Terms*—Blackout, cascading failure, coupled interaction model, coupled interaction network, interdependency, line outage, load shed, outage propagation, risk mitigation.**

I. Introduction

CASCADING failure is one of the dominant causes of blackouts. Although initiating outages usually only involve a small number of components, the failure can propagate in a large area of the transmission system and may lead to a significant amount of load shed [1], [2]. Cascading failure has been widely studied by using physical simulation models, which include OPA model [3] and its variants [4], [5], Manchester model [6], COSMIC model [7], Multi-Timescale Quasi-Dynamic Model [8], the model with detailed protection systems [9], and the AC power flow based model that explicitly considers temperature disturbance and the system response [10]. These models mainly differ from each other in the physical mechanisms that are considered [11]. Although acceleration techniques, such as Random Chemistry algorithm [12], importance sampling [13], and simplified power flow calculation [14], have been proposed, physical simulation models usually require a high computational cost due to the complicated mechanisms.

L. Wang, B. Hu, and K. Xie's work was supported by National Natural Science Foundation of China under Grants 51725701 and 51861145406. The work of Junjian Qi was supported by the National Science Foundation under Grant CAREER 2110211. Paper no. TPWRS-01157-2020. *(Corresponding author: Bo Hu.)*

L. Wang is with the Department of Electrical Engineering, Chongqing University, Chongqing 400044 China and was with the Department of Electrical and Computer Engineering, Stevens Institute of Technology, Hoboken, NJ 07030 USA (e-mail: leibaowang1993@163.com).

J. Qi is with the Department of Electrical and Computer Engineering, Stevens Institute of Technology, Hoboken, NJ 07030 USA (e-mail: jqi8@stevens.edu).

B. Hu and K. Xie are with the Department of Electrical Engineering, Chongqing University, Chongqing 400044 China (e-mails: hboy8361@163.com; kaiguixie@vip.163.com).

Different from physical simulation models, complex network based models ignore most physical properties and analyze power system vulnerability only based on the network structure. For example, degree distribution [15] and structural index [16] are used as robustness measures of the power system against blackouts. Cascading failure behaviors have also been extensively studied in the sandpile model on different types of complex networks [17], [18]. Although the complex network based methods require a much lower computational time, it is difficult to incorporate the physical mechanisms of cascading failure into the topological metrics.

Due to the limitations of the physical simulation models and complex network based approaches, high-level statistical models such as branching processes [19]–[22] have been proposed to extract useful information from either simulated cascades or utility outage data. Branching process is introduced to model the propagation of line outages and efficiently estimate the distribution of the number of line outages in [19], [23]. The propagation of load shed is also analyzed with branching process [20], [21]. In [22], the interdependencies between different types of outages are analyzed by multi-type branching process. Although branching process can capture the distribution of line outages and the load shed, it does not distinguish components that fail in cascading failure propagation, and thus cannot identify critical components for cascading mitigation.

Besides, the recent studies on interaction network [24]–[27] and influence graph [28]–[30] provide another more useful way to extract propagation patterns in the original cascades. In [25], the estimation of the interaction network for line outages is formulated as a parameter estimation problem with incomplete data and is efficiently solved with the Expectation Maximization (EM) algorithm. Influence graphs are constructed by Markovian process in [28]–[30], in which the transition probability is estimated by Bayesian inferring [30]. In addition to line outages, the load shed and electrical distances are also analyzed by a multi-layer interaction graph in [26]. Although the load shed is considered as one layer, the cause of the load shed at buses is equally distributed to the failed lines, which may not always be reasonable as the contribution of line outages to the load shed can be significantly different.

Although the existing high-level statistical models provide useful tools to capture the pattern of outage propagation, it is still very challenging to analyze the interaction between line outages and the load shed, especially with limited samples. In this paper, we aim at addressing this challenge by revealing the pattern of interactions between line outages and the load shed and further developing effective cascading failure mitigation strategies based on the proposed coupled interaction matrix and coupled interaction model. The major contributions of this paper are summarized as follows.

1) A coupled interaction matrix is proposed to describe the interactions between line outages and the load shed at buses, and is efficiently estimated by the EM algorithm with a small number of original cascades.
2) A coupled interaction model that utilizes the coupled interaction matrix and the distribution of initial outages is proposed to efficiently simulate cascading failures with both line outages and the load shed at buses.
3) Critical links are identified with the interaction matrix based on a defined comprehensive severity index that considers the consequences of both line outages and the load shed. The critical link based mitigation strategy is implemented and is shown to be able to significantly reduce both line outages and the load shed.

The remainder of this paper is organized as follows. Section II defines the coupled interaction matrix. Section III estimates the coupled interaction matrix by the EM algorithm. Section IV proposes a coupled interaction model for efficient cascading failure simulation based on the estimated interaction matrix. Section V develops a method to identify critical links based on a comprehensive severity index. Section VI validates the effectiveness of the proposed approach on the IEEE 300-bus system. Finally, conclusions are drawn in Section VII.

II. Coupled Interaction Matrix

Cascading failures in power systems involve successive line outages and load shed at buses. According to the outage sequence from either the utility outage record [19] or cascading failure simulations [24], a cascade can be divided into different generations. Assume there are N_l lines and N_b buses with load in the system. The index numbers of lines and load buses are converted so that the set of lines is $\{1, 2, \cdots, N_l\}$ and the set of buses with load is $\{1, 2, \cdots, N_b\}$. Assume there are M cascades in the dataset as shown below:

	generation 0	generation 1	generation 2	...
cascade 1	$\mathcal{F}^{1,0}$	$\mathcal{F}^{1,1}$	$\mathcal{F}^{1,2}$	...
$\vdots$	$\vdots$	$\vdots$	$\vdots$	$\vdots$
cascade m	$\mathcal{F}^{m,0}$	$\mathcal{F}^{m,1}$	$\mathcal{F}^{m,2}$	...
$\vdots$	$\vdots$	$\vdots$	$\vdots$	$\vdots$
cascade M	$\mathcal{F}^{M,0}$	$\mathcal{F}^{M,1}$	$\mathcal{F}^{M,2}$	...

where $\mathcal{F}^{m,g} = \{\mathcal{S}_{\mathsf{L}}^{m,g}, \mathcal{S}_{\mathsf{B}}^{m,g}, \boldsymbol{Z}^{m,g}\}$, $\mathcal{S}_{\mathsf{L}}^{m,g}$ and $\mathcal{S}_{\mathsf{B}}^{m,g}$ are, respectively, the set of lines that outage and the set of buses with load shed in generation g of cascade m, and $\boldsymbol{Z}^{m,g} \in \mathbb{Z}^{N_b}$ is the vector for the amount of discretized load shed at each bus in generation g of cascade m.

In both utility outage data and cascading failure simulations, the load shed is usually recorded in MW. Let $X_v^{m,g}$ be the load shed at bus v in MW in generation g of cascade m. Discretization should be first performed on the load shed data by the technique in [21], [22]. If Δ_v MW is the chosen unit of discretization for bus v, an integer multiples of Δ_v MW can be obtained for the load shed at bus v as

$$Z_v^{m,g} = \mathrm{int}\left[\frac{X_v^{m,g}}{\Delta_v} + 0.5\right], \tag{1}$$

where $\mathrm{int}[x]$ is the integer part of x. A systematic approach for choosing Δ_v will be discussed in Section III.

The interaction model in [24] and [25] only focuses on the propagation of line outages. In this paper the interaction analysis is not only for line outages but also considers the interdependency between line outages and the load shed at different buses. This is useful because the load shed corresponds to more direct economic losses and is of more interest by the utilities. The analysis of interactions between line outages and the load shed at buses enables better capture of the cascading failure propagation patterns and can help develop more effective mitigation strategies.

A. *Definition of Coupled Interaction Matrix* $\boldsymbol{B}$

In order to capture the interdependency between line outages and the load shed, a coupled interaction matrix $\boldsymbol{B} \in \mathbb{R}^{(N_l+N_b)\times(N_l+N_b)}$ is defined as

$$\boldsymbol{B} = \begin{bmatrix} \boldsymbol{B}^{\mathsf{LL}} & \boldsymbol{B}^{\mathsf{LB}} \\ \boldsymbol{B}^{\mathsf{BL}} & \boldsymbol{B}^{\mathsf{BB}} \end{bmatrix},$$

where $\boldsymbol{B}^{\mathsf{LL}}$, $\boldsymbol{B}^{\mathsf{LB}}$, $\boldsymbol{B}^{\mathsf{BL}}$, and $\boldsymbol{B}^{\mathsf{BB}}$ are defined as follows. Throughout the paper we assume that $M_{\mathrm{u}} \leq M$ cascades are used for estimating the coupled interaction matrix.

- $\boldsymbol{B}^{\mathsf{LL}} \in \mathbb{R}^{N_l\times N_l}$ captures the interactions between lines outages, which is the same as the interaction matrix in [24] and [25]. Its entry in the ith row and jth column, b_{ij}^{LL}, is the empirical probability that line j fails following the outage of line i.
- $\boldsymbol{B}^{\mathsf{LB}} \in \mathbb{R}^{N_l\times N_b}$ captures the interactions from line outages to the load shed at buses. As has been adopted and verified in [20]–[22], Poisson distribution can capture the statistical properties for offspring outages being selected from a large number of possible outages that have small probability and are approximately independent. Therefore, we use Poisson distribution to approximate the distribution of the discretized load shed at buses following line outages. For example, to capture the discretized load shed at bus v following the outage of line i, the mean of Poisson distribution is recorded as b_{iv}^{LB}, which is the entry in the ith row and vth column of $\boldsymbol{B}^{\mathsf{LB}}$. If line i fails in generation g, k_v units of discretized load shed at bus v will occur in generation $g+1$ with probability

$$p_{iv}^{\mathsf{LB}} = \frac{\left(b_{iv}^{\mathsf{LB}}\right)^{k_v}}{k_v!} e^{-b_{iv}^{\mathsf{LB}}}. \tag{2}$$

- $\boldsymbol{B}^{\mathsf{BL}} \in \mathbb{R}^{N_b\times N_l}$ captures the interactions from the load shed to line outages. Note that in this paper the interactions between the load shed at buses and the further line outages are not necessarily causal, but actually capture what might consequently happen in the next generation following the load shedding event in current generation.

When load shedding cannot eliminate all line overloading or other technical constraint violations [31], [32], line outages can still be observed following the load shedding event. As has been verified in [22], line outages following load shedding are rare. Therefore, we consider a simplified case in which line outages are not sensitive to the amount of load shed at buses. When load shedding occurs at bus u, line j will fail in the next generation with a constant probability b_{uj}^{BL}, which is the entry in the uth row and jth column of $\boldsymbol{B}^{\mathsf{BL}}$.

- $\boldsymbol{B}^{\mathsf{BB}} \in \mathbb{R}^{N_b \times N_b}$ captures the interactions between the load shed at buses. Similar to $\boldsymbol{B}^{\mathsf{BL}}$, $\boldsymbol{B}^{\mathsf{BB}}$ captures the successive load shedding in consecutive generations that is also not necessarily causal. As the system has been significantly weakened when the cascading outage evolves, successive load shedding may occur at different buses or at the same bus more than once. We assume each unit of the discretized load shed at bus u independently generates the discretized load shed at bus v by a Poisson distribution with mean b_{uv}^{BB}. Therefore, if k_u units of load are shed at bus u in generation g, k_v units of discretized load shed at bus v will occur in generation $g+1$ with the following probability:

$$p_{uv}^{\mathsf{BB}} = \frac{\left(k_u b_{uv}^{\mathsf{BB}}\right)^{k_v}}{k_v!} e^{-k_u b_{uv}^{\mathsf{BB}}}. \tag{3}$$

The matrix $\boldsymbol{B}$ determines how components, either lines or buses, interact with each other. The nonzero entries of $\boldsymbol{B}$ are called links. Link $l: i \to j$ corresponds to $\boldsymbol{B}$'s nonzero entry in the ith row and jth column. By putting all links together a directed network $\mathcal{G}(\mathcal{C}, \mathcal{L})$ called *coupled interaction network* can be obtained: the vertices $\mathcal{C}$ are components, including both lines and buses, and the directed link $l \in \mathcal{L}$ represents that the destination vertex component fails following the source vertex component outage with probability greater than 0. Different from [24], [25], there are four different types of links: $\mathsf{L} \to \mathsf{L}$ links, $\mathsf{L} \to \mathsf{B}$ links, $\mathsf{B} \to \mathsf{L}$ links, and $\mathsf{B} \to \mathsf{B}$ links.

B. Definition of Auxiliary Matrix $\boldsymbol{A}$

To estimate the coupled interaction matrix $\boldsymbol{B}$, the following auxiliary matrix $\boldsymbol{A} \in \mathbb{R}^{(N_l+N_b)\times(N_l+N_b)}$ is needed:

$$\boldsymbol{A} = \begin{bmatrix} \boldsymbol{A}^{\mathsf{LL}} & \boldsymbol{A}^{\mathsf{LB}} \\ \boldsymbol{A}^{\mathsf{BL}} & \boldsymbol{A}^{\mathsf{BB}} \end{bmatrix},$$

whose four sub-matrices are defined below.

- $\boldsymbol{A}^{\mathsf{LL}} \in \mathbb{R}^{N_l \times N_l}$ has entry a_{ij}^{LL} as the total number of times that line j fails following the outage of line i in the dataset. Based on a_{ij}^{LL}, b_{ij}^{LL} can be estimated as

$$b_{ij}^{\mathsf{LL}} = \frac{a_{ij}^{\mathsf{LL}}}{N_i^{\mathsf{L}}}, \tag{4}$$

where N_i^{L} is the total number of outages of line i in the M_{u} cascades.

- $\boldsymbol{A}^{\mathsf{LB}} \in \mathbb{R}^{N_l \times N_b}$ has entry a_{iv}^{LB} as the total discretized amount of load shed at bus v following the outage of line i in the M_{u} cascades. Then b_{iv}^{LB} can be estimated by

$$b_{iv}^{\mathsf{LB}} = \frac{a_{iv}^{\mathsf{LB}}}{N_i^{\mathsf{L}}}. \tag{5}$$

- $\boldsymbol{A}^{\mathsf{BL}} \in \mathbb{R}^{N_b \times N_l}$ has entry a_{uj}^{BL} as the total number of outages of line j following the load shed at bus u, from which b_{uj}^{BL} is estimated as

$$b_{uj}^{\mathsf{BL}} = \frac{a_{uj}^{\mathsf{BL}}}{N_u^{\mathsf{B}}}, \tag{6}$$

where N_u^{B} is the total number of times that bus u has nonzero discretized load shed in the M_{u} cascades.

- $\boldsymbol{A}^{\mathsf{BB}} \in \mathbb{R}^{N_b \times N_b}$ has entry a_{uv}^{BB} as the total discretized amount of load shed at bus v following the load shed at bus u. As the load shed at bus v after each unit of load shed at bus u independently follows Poisson distribution, whose mean b_{uv}^{BB} can be estimated by

$$b_{uv}^{\mathsf{BB}} = \frac{a_{uv}^{\mathsf{BB}}}{\sum_{m=1}^{M_{\mathrm{u}}} \sum_{g=0}^{G^m-1} Z_u^{m,g}}, \tag{7}$$

where G^m is the number of generations in cascade m and the denominator is the total discretized amount of load shed at bus u in the M_{u} cascades.

III. Estimating Coupled Interaction Matrix by EM Algorithm

When there are multiple line outages and the load shed at multiple buses in two successive generations, it is challenging to decide the actual interactions between outages, either line outages or the load shed, and further determine $\boldsymbol{A}$ and $\boldsymbol{B}$. To address this issue, this paper adopts the EM algorithm to infer the interactions between outages [22], [25], [33]. The EM algorithm iterates over E-step and M-step to maximize the likelihood estimation of the coupled interaction matrix $\boldsymbol{B}$ until convergence. Moreover, as the capability of Poisson distribution to capture the propagation of load shed can be improved by the choice of the discretization unit Δ_v [21], the discretization units for load buses are also adaptively updated with the EM algorithm. The detailed procedure is as follows.

1) *Initialization of discretization units*: An initial discretization unit $\Delta_v^{(0)} = 50$ MW is chosen for each load bus v. The load shed at buses in the original M_{u} cascades is processed by (1) with the initial discretization units.
2) *Initialization of $\boldsymbol{A}$ and $\boldsymbol{B}$*: Each component in generation $g+1$ is initially assumed to follow each outage in generation g. An initial matrix $\boldsymbol{A}^{(0)}$ can thus be constructed by processing the original M_{u} cascades, based on which the initial $\boldsymbol{B}^{(0)}$ can be calculated by (4)–(7).
3) *E-step*: Update $\boldsymbol{A}^{(k+1)}$ based on $\boldsymbol{B}^{(k)}$
   In the $(k+1)$th iteration, $p_{ij}^{m,g(k+1)}$ and $p_{uj}^{m,g(k+1)}$, the probability of line j outage in generation $g+1$ following line i outage and that following the load shed at bus u in generation g of cascade m, are estimated as:

$$p_{ij}^{m,g(k+1)} = \frac{b_{ij}^{\mathsf{LL}(k)}}{1 - \prod_{c\in\mathcal{S}_{\mathsf{L}}^{m,g}} \left(1 - b_{cj}^{\mathsf{LL}(k)}\right) \prod_{c\in\mathcal{S}_{\mathsf{B}}^{m,g}} \left(1 - b_{cj}^{\mathsf{BL}(k)}\right)}$$

$$p_{uj}^{m,g(k+1)} = \frac{b_{uj}^{\mathsf{BL}(k)}}{1 - \prod_{c\in\mathcal{S}_{\mathsf{L}}^{m,g}} \left(1 - b_{cj}^{\mathsf{LL}(k)}\right) \prod_{c\in\mathcal{S}_{\mathsf{B}}^{m,g}} \left(1 - b_{cj}^{\mathsf{BL}(k)}\right)}.$$

Similarly, $p_{iv}^{m,g(k+1)}$ and $p_{uv}^{m,g(k+1)}$, the probability of having $Z_v^{m,g+1}$ units of discretized load shed at bus v in generation $g+1$ following the outage of line i and that following the load shed at bus u in generation g of cascade m, are estimated as:

$$p_{iv}^{m,g(k+1)} = \frac{p_{iv}^{\mathsf{LB}(k)}}{1 - \prod_{c\in\mathcal{S}_{\mathsf{L}}^{m,g}} \left(1 - p_{cv}^{\mathsf{LB}(k)}\right) \prod_{c\in\mathcal{S}_{\mathsf{B}}^{m,g}} \left(1 - p_{cv}^{\mathsf{BB}(k)}\right)}$$

$$p_{uv}^{m,g(k+1)} = \frac{p_{uv}^{\mathsf{BB}(k)}}{1 - \prod_{c\in\mathcal{S}_{\mathsf{L}}^{m,g}} \left(1 - p_{cv}^{\mathsf{LB}(k)}\right) \prod_{c\in\mathcal{S}_{\mathsf{B}}^{m,g}} \left(1 - p_{cv}^{\mathsf{BB}(k)}\right)},$$

where $p_{iv}^{\mathsf{LB}(k)}$ and $p_{uv}^{\mathsf{BB}(k)}$ can be calculated by (2)–(3) based on $\boldsymbol{B}^{(k)}$.

The entries of $\boldsymbol{A}^{\mathsf{LL}}$ and $\boldsymbol{A}^{\mathsf{BL}}$ are updated as

$$a_{ij}^{\mathsf{LL}(k+1)} = \sum_{m=1}^{M_{\mathrm{u}}} \sum_{g=0}^{G^m-2} p_{ij}^{m,g(k+1)} \tag{8}$$

$$a_{uj}^{\mathsf{BL}(k+1)} = \sum_{m=1}^{M_{\mathrm{u}}} \sum_{g=0}^{G^m-2} p_{uj}^{m,g(k+1)}, \tag{9}$$

where $p_{ij}^{m,g(k+1)}$ is zero if line $i \notin \mathcal{S}_{\mathsf{L}}^{m,g}$ or line $j \notin \mathcal{S}_{\mathsf{L}}^{m,g+1}$. And $p_{uj}^{m,g(k+1)}$ is zero if bus $u \notin \mathcal{S}_{\mathsf{B}}^{m,g}$ or line $j \notin \mathcal{S}_{\mathsf{L}}^{m,g+1}$.

The entries of $\boldsymbol{A}^{\mathsf{LB}}$ and $\boldsymbol{A}^{\mathsf{BB}}$ are updated as

$$a_{iv}^{\mathsf{LB}(k+1)} = \sum_{m=1}^{M_{\mathrm{u}}} \sum_{g=0}^{G^m-2} Z_v^{m,g+1} p_{iv}^{m,g(k+1)} \tag{10}$$

$$a_{uv}^{\mathsf{BB}(k+1)} = \sum_{m=1}^{M_{\mathrm{u}}} \sum_{g=0}^{G^m-2} Z_v^{m,g+1} p_{uv}^{m,g(k+1)}, \tag{11}$$

where $p_{iv}^{m,g(k+1)}$ is zero if line $i \notin \mathcal{S}_{\mathsf{L}}^{m,g}$ or bus $v \notin \mathcal{S}_{\mathsf{B}}^{m,g+1}$. And $p_{uv}^{m,g(k+1)}$ is zero if bus $u \notin \mathcal{S}_{\mathsf{B}}^{m,g}$ or bus $v \notin \mathcal{S}_{\mathsf{B}}^{m,g+1}$.

The interactions of the load shed following line outages are also recorded to update the discretization units. Take the load shed at bus v following the outages of line i as an example. First let U_v denote the maximum amount of discretized load shed at bus v. Let the vector $\boldsymbol{C}_{iv}^{\mathsf{LB}(k+1)} \in \mathbb{R}^{U_v+1}$ record the number of cumulative times of the load shed at bus v following the N_i^{L} times of the outage of line i in M_u cascades. For the nth outage of line i, if there is no discretized load shed at bus v, $C_{iv}^{\mathsf{LB}(k+1)}(0)$ increases by 1. Otherwise, if $Z_v^{m,g+1}$ units of discretized load shed at bus v follow the nth outage of line i with a probability of $p_{iv}^{m,g(k+1)}$, $C_{iv}^{\mathsf{LB}(k+1)}(0)$ and $C_{iv}^{\mathsf{LB}(k+1)}(Z_v^{m,g+1})$ increase by $1 - p_{iv}^{m,g(k+1)}$ and $p_{iv}^{m,g(k+1)}$, respectively.

4) *M-step*: Update $\boldsymbol{B}^{(k+1)}$ based on $\boldsymbol{A}^{(k+1)}$

4.1) The estimation of interaction matrix $\tilde{\boldsymbol{B}}^{(k+1)} \in \mathbb{R}^{(N_l+N_b)\times(N_l+N_b)}$ is updated with $\boldsymbol{A}^{(k+1)}$ according to (4)–(7).

4.2) The sample variance of the discretized load shed at bus v following the outage of line i is calculated as:

$$S_{iv}^{2(k+1)} = \frac{\sum_{l=0}^{U_v} C_{iv}^{\mathsf{LB}(k+1)}(l)\left(l - \tilde{b}_{iv}^{\mathsf{LB}(k+1)}\right)^2}{N_i^{\mathsf{L}} - 1}. \tag{12}$$

4.3) For each load bus v, Δ_v is updated as:

$$\Delta_v^{(k+1)} = \Delta_v^{(k)} \sqrt{\frac{\sum_{i\in\mathcal{S}_v^{\mathsf{LB}}} N_i^{\mathsf{L}} \frac{S_{iv}^{2(k+1)}}{\tilde{b}_{iv}^{\mathsf{LB}(k+1)}}}{\sum_{i\in\mathcal{S}_v^{\mathsf{LB}}} N_i^{\mathsf{L}} \frac{\tilde{b}_{iv}^{\mathsf{LB}(k+1)}}{S_{iv}^{2(k+1)}}}}, \tag{13}$$

where $\mathcal{S}_v^{\mathsf{LB}}$ is the set of row indices at which the vth column of $\tilde{\boldsymbol{B}}^{\mathsf{LB}(k+1)}$ has nonzero entries. More detailed explanation of (13) can be found in the Appendix.

4.4) Using the updated discretization units, the load shed at buses in the original M_{u} cascades is reprocessed by (1). And the entries in $\boldsymbol{B}^{\mathsf{LB}(k+1)}$ and $\boldsymbol{B}^{\mathsf{BB}(k+1)}$ are updated from $\tilde{\boldsymbol{B}}^{\mathsf{LB}(k+1)}$ and $\tilde{\boldsymbol{B}}^{\mathsf{BB}(k+1)}$ as:

$$b_{iv}^{\mathsf{LB}(k+1)} = \frac{\Delta_v^{(k)}}{\Delta_v^{(k+1)}} \tilde{b}_{iv}^{\mathsf{LB}(k+1)} \tag{14}$$

$$b_{uv}^{\mathsf{BB}(k+1)} = \frac{\Delta_u^{(k+1)}\Delta_v^{(k)}}{\Delta_u^{(k)}\Delta_v^{(k+1)}} \tilde{b}_{uv}^{\mathsf{BB}(k+1)}. \tag{15}$$

5) *End*: Steps 3–5 are repeated until the following condition is satisfied:

$$\sigma_{\boldsymbol{B}} = \sqrt{\frac{\sum_{i=1}^{N_l+N_b} \sum_{j=1}^{N_l+N_b} \left(b_{ij}^{(k+1)} - b_{ij}^{(k)}\right)^2}{N}} \le \varepsilon, \tag{16}$$

where $N = N_{\neq 0}$ if $N_{\neq 0}$, the number of nonzero entries in $\boldsymbol{B}^{(k+1)} - \boldsymbol{B}^{(k)}$, is greater than 0, otherwise $N = 1$, and ε is the preset threshold.

After the convergence of the EM algorithm, the estimated matrix $\boldsymbol{B}$ and the discretization units in the last iteration will be used for the cascading outage simulation in Section IV and mitigation in Section V.

IV. Coupled Interaction Model for Cascading Failure Simulation

As large blackouts are usually rare, simulating large blackouts with physical cascading failure models is rather inefficient, while the number of available utility outage data sample is limited. By contrast, highly probabilistic interaction models [24], [27], [30] can efficiently generate a large number of cascades to better estimate the blackout size [34]. Moreover, the effect of mitigation schemes can also be efficiently tested by modifying the parameters of highly probabilistic models. In this section, a coupled interaction model is proposed to simulate the propagation of line outages and the load shed utilizing the probability distribution of initial outages and the coupled interaction matrix $\boldsymbol{B}$. The coupled interaction model has the following four steps.

- *Step 1: Generate initial outages*

  Set $g = 0$. The line outages in generation 0 are independently generated according to their occurrence frequency in generation 0 of the original cascades. Specifically, line i fails in generation 0 by probability:

$$\pi_i^{\mathsf{L}} = \frac{\sum_{m=1}^{M_{\mathrm{u}}} \mathbf{1}\big[i \in \mathcal{S}_{\mathsf{L}}^{m,0}\big]}{M_{\mathrm{u}}}, \tag{17}$$

where $\mathbf{1}[\text{event}]$ is an indicator function that evaluates to one if the event happens and evaluates to zero when the event does not happen.

Similarly, bus u has k units of discretized load shed in generation 0 by probability:

$$\pi_{u,k}^{\mathsf{B}} = \frac{\sum_{m=1}^{M_{\mathrm{u}}} \mathbf{1}[Z_u^{m,0} = k]}{M_{\mathrm{u}}}. \tag{18}$$

All generated outages comprise $\mathcal{S}_{\mathsf{L}}^{m,0}$, $\mathcal{S}_{\mathsf{B}}^{m,0}$, and $\boldsymbol{Z}^{m,0}$. Considering the time scale of cascading failures, most cascading failure simulation models do not include any repair process of the failed lines. As each line fails at most once in a simulation, once line i fails the entries in the ith column of $\boldsymbol{B}^{\mathsf{LL}}$ and $\boldsymbol{B}^{\mathsf{BL}}$ are set to be zero.

- *Step 2: Generate further line outages*

  Each outage in $\mathcal{S}_{\mathsf{L}}^{m,g}$ and $\mathcal{S}_{\mathsf{B}}^{m,g}$ independently generates line outages in generation $g+1$. Line j fails in generation $g+1$ following line i outage in $\mathcal{S}_{\mathsf{L}}^{m,g}$ and the load shed at bus u in $\mathcal{S}_{\mathsf{B}}^{m,g}$ with probability b_{ij}^{LL} and b_{uj}^{BL}, respectively. All sampled line outages comprise $\mathcal{S}_{\mathsf{L}}^{m,g+1}$. The columns of $\boldsymbol{B}^{\mathsf{LL}}$ and $\boldsymbol{B}^{\mathsf{BL}}$ that are corresponding to the failed lines are set to be zero.

- *Step 3: Generate further load shed*

  For line $i \in \mathcal{S}_{\mathsf{L}}^{m,g}$, the discretized load shed at bus v follows Poisson distribution with mean b_{iv}^{LB}. For bus $u \in \mathcal{S}_{\mathsf{B}}^{m,g}$, the discretized load shed at bus v follows Poisson distribution with mean $Z_u^{m,g} b_{uv}^{\mathsf{BB}}$. The load shed at bus v are independently sampled for each outage in $\mathcal{S}_{\mathsf{L}}^{m,g}$ and $\mathcal{S}_{\mathsf{B}}^{m,g}$. Since the total load shed at bus v from generation 0 to $g+1$ cannot exceed its total discretized load Z_v^{t}, the load shed at bus v in generation $g+1$ is recorded as $Z_v^{m,g+1} = \min\big\{Z_v^{\mathrm{t}} - \sum_{l=0}^{g} Z_v^{m,l}, \sum_{i\in\mathcal{S}_{\mathsf{L}}^{m,g}} Z_{v\leftarrow i}^{m,g+1} + \sum_{u\in\mathcal{S}_{\mathsf{B}}^{m,g}} Z_{v\leftarrow u}^{m,g+1}\big\}$, where $Z_{v\leftarrow i}^{m,g+1}$ and $Z_{v\leftarrow u}^{m,g+1}$ are the load shed at bus v in generation $g+1$ generated from line outage i and the load shed at bus u, respectively. All buses with load shed comprise $\mathcal{S}_{\mathsf{B}}^{m,g+1}$ and the corresponding discretized load shed is recorded in $\boldsymbol{Z}^{m,g+1}$.

- *Step 4: End*

  Simulation ends if both $\mathcal{S}_{\mathsf{L}}^{m,g+1}$ and $\mathcal{S}_{\mathsf{B}}^{m,g+1}$ are empty. Otherwise, increase g by one and go back to Step 2.

Steps 1–4 can be repeated to simulate many cascades for better understanding and mitigating cascading failures. Compared with detailed cascading failure models, the coupled interaction model is highly probabilistic and is thus much more time-efficient, which will be validated in Section VI-B.

V. Critical Link Identification

As both the number of line outages and the amount of load shed have been used as the measures of blackout size [34], the mitigation effect of cascading outages can also be measured by the comprehensive cost of line outages and the load shed. In this paper, the severity of a link $l : S \rightarrow T$ is measured by the line outages and load shed propagated through l, where S and T are, respectively, the source outage and target outage and could be a line outage or a bus with load shedding. For each link $l : S \rightarrow T$, an acyclic interaction subgraph $\mathcal{G}_l(\mathcal{C}_l, \mathcal{L}_l)$ in which there is a path from vertex T to any other vertex can be obtained from the coupled interaction network.

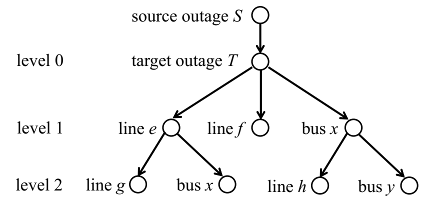

Fig. 1. Illustration of an interaction subgraph starting with link $l : S \rightarrow T$.

As a line cannot outage twice in one propagation path while a bus may have load shedding for multiple times in one path, different vertices in the subgraph $\mathcal{G}_l(\mathcal{C}_l, \mathcal{L}_l)$ cannot represent the same line outage event but can be load shedding events at the same bus. To extract the acyclic subgraph, the links to a vertex as line outage event from other vertices at the same or higher levels are removed as in [24]. For the link to a vertex as load shedding event from other vertices at the same or higher levels, we remove the link, add a new vertex for the load shedding event at the next level of the source vertex of the removed link, and connect the source vertex of the removed link to the newly added vertex. This eliminates the loops in the original subgraph by adding the vertices for the load shedding events at the same buses at multiple levels.

Fig. 1 shows an example of such an acyclic interaction subgraph. In the coupled interaction network, the load shedding at bus x follows both the target outage T at level 0 and the line e outage at level 1. To capture the load shedding at bus x in the propagation path, a new vertex is added at level 2 for the load shedding event at bus x. With the interaction subgraph, the severity index for link l can be calculated as follows.

- *Step 1: Estimate the expected number of outages of T*
  - When S denotes line i outage and T denotes line j outage, given the total number of line i outage in the M_{u} cascades as N_i^{L}, the expected value of the number of line j outage following line i outage is estimated as:

    $$E_j^{\mathsf{L}} = N_i^{\mathsf{L}} b_{ij}^{\mathsf{LL}}. \tag{19}$$

  - When S denotes line i outage and T denotes the load shed at bus v, the expected value of the amount of load shed at bus v at level 0 is estimated as:

    $$E_v^{\mathsf{B},0} = N_i^{\mathsf{L}} b_{iv}^{\mathsf{LB}} \Delta_v. \tag{20}$$

    The number of times of load shedding at bus v at level 0 following line i outage is estimated as:

    $$\hat{N}_v^{\mathsf{B},0} = N_i^{\mathsf{L}} \big(1 - e^{-b_{iv}^{\mathsf{LB}}}\big), \tag{21}$$

where $\left(1-e^{-b_{iv}^{\mathsf{LB}}}\right)$ is the probability of having nonzero events for a Poisson distribution with mean b_{iv}^{LB}.

– When S denotes the load shed at bus u and T denotes line j outage, given the total number of times that bus u has load shedding in the $M_{\rm u}$ cascades as N_u^{B}, the expected value of the number of line j outage is estimated as:

$$E_j^{\mathsf{L}} = N_u^{\mathsf{B}} b_{uj}^{\mathsf{BL}}. \tag{22}$$

– When S denotes the load shed at bus u and T denotes the load shed at bus v, the expected value of the amount of load shed at bus v at level 0 is estimated as:

$$E_v^{\mathsf{B},0} = \sum_{m=1}^{M_{\rm u}} \sum_{g=0}^{G^m-1} Z_u^{m,g} b_{uv}^{\mathsf{BB}} \Delta_v. \tag{23}$$

The expected value of the number of times of load shedding at bus v at level 0 following the load shed at bus u is estimated as:

$$\hat{N}_v^{\mathsf{B},0} = \sum_{m=1}^{M_{\rm u}} \sum_{g=0}^{G^m-1} \left(1 - e^{-Z_u^{m,g} b_{uv}^{\mathsf{BB}}}\right), \tag{24}$$

where $\left(1-e^{-Z_u^{m,g} b_{uv}^{\mathsf{BB}}}\right)$ is the probability of observing nonzero load shed at bus v following the load shed of $Z_u^{m,g}$ at bus u.

- *Step 2: Estimate the expected value of the outages at level 1 based on the expected value of outage T and $\boldsymbol{B}$*

– When T denotes line j outage, the expected value of the outage of line e at level 1 can be estimated by

$$E_e^{\mathsf{L}} = E_j^{\mathsf{L}} b_{je}^{\mathsf{LL}}. \tag{25}$$

The expected value of the amount of load shed at bus x at level 1 can be estimated by:

$$E_x^{\mathsf{B},1} = E_j^{\mathsf{L}} b_{jx}^{\mathsf{LB}} \Delta_x, \tag{26}$$

and the expected value of the number of times of load shedding at bus x at level 1 is:

$$\hat{N}_x^{\mathsf{B},1} = E_j^{\mathsf{L}} \left(1 - e^{-b_{jx}^{\mathsf{LB}}}\right). \tag{27}$$

– When T denotes the load shed at bus v, the expected value of the number of outage of line e at level 1 can be estimated as:

$$E_e^{\mathsf{L}} = \hat{N}_v^{\mathsf{B},0} b_{ve}^{\mathsf{BL}}. \tag{28}$$

The load shed at bus x at level 1 following outage T as the load shed at bus v can be estimated as:

$$E_x^{\mathsf{B},1} = \frac{E_v^{\mathsf{B},0}}{\Delta_v} b_{vx}^{\mathsf{BB}} \Delta_x, \tag{29}$$

and the expected value of the number of times of load shedding at bus x at level 1 is:

$$\hat{N}_x^{\mathsf{B},1} = \hat{N}_v^{\mathsf{B},0} \left(1 - e^{-\frac{E_v^{\mathsf{B},0} b_{vx}^{\mathsf{BB}}}{\hat{N}_v^{\mathsf{B},0} \Delta_v}}\right), \tag{30}$$

where $\left(1 - e^{-E_v^{\mathsf{B},0} b_{vx}^{\mathsf{BB}} / (\hat{N}_v^{\mathsf{B},0} \Delta_v)}\right)$ is the probability of having positive load shed at bus x, in which the discretized amount of load shed at bus v at level 0 in one of the $\hat{N}_v^{\mathsf{B},0}$ load shedding is approximated by its average value $E_v^{\mathsf{B},0} / (\hat{N}_v^{\mathsf{B},0} \Delta_v)$.

- *Step 3: Estimate the expected value of the outages at higher levels*

  The expected value of the outages at level $k \geq 2$ can also be calculated with the estimated outages at level $k-1$, which is similar to the calculations in Step 2.

- *Step 4: Calculate the comprehensive severity index I_l*

  To measure the total number of line outages propagated through link l, the severity index I_l^{L} is calculated as:

$$I_l^{\mathsf{L}} = \sum_{c \in \mathcal{C}_l^{\mathsf{L}}} E_c^{\mathsf{L}}, \tag{31}$$

  where $\mathcal{C}_l^{\mathsf{L}}$ is the set of lines at all levels of the interaction subgraph starting with link l.

  To measure the total amount of load shed propagated through link l, the severity index I_l^{B} is calculated as:

$$I_l^{\mathsf{B}} = \sum_{k=0}^{K-1} \sum_{c \in \mathcal{C}_l^{\mathsf{B},k}} E_c^{\mathsf{B},k}, \tag{32}$$

  where K is the number of levels in the subgraph and $\mathcal{C}_l^{\mathsf{B},k}$ is the set of buses at level k of the interaction subgraph starting with link l.

  Then a comprehensive severity index I_l is calculated as:

$$I_l = c^{\mathsf{L}} \frac{I_l^{\mathsf{L}}}{N_l} + c^{\mathsf{B}} \frac{I_l^{\mathsf{B}}}{X^{\rm t}}, \tag{33}$$

  where c^{L} and c^{B} are the cost coefficients for line outages and load shed set by the operators of the system, and $X^{\rm t}$ is the total load of the system in MW.

Based on the ranking of I_l, critical links can be identified from the perspective of consequences in both line outages and the load shed. Note that the severity index I_l is only considering the cost of the load shed (line outages) when c^{L} (c^{B}) is set as zero. In practical application, the ratio between c^{L} and c^{B} can be adjusted by the operators according to their preference or the actual costs of line outages and the load shed. Mitigation strategies can further be implemented based on the identified critical links to reduce the risk of blackouts, which will be discussed in Sections VI-C and VI-D.

VI. Simulation Results

In this section, the proposed method is validated on the IEEE 300-bus system [35]. This system has 191 buses with load and 411 lines. The total load and total generation capacity are, respectively, 23,848 MW and 32,678 MW. The open-loop OPA [3] is adopted to generate 30,000 original cascades. The parameters of the OPA model in [3] are set as $\gamma = 2$, $\alpha = 0.95$, $\beta = 0.30$, and $p_0 = 0.001$. The initialization of the discretization units in the EM algorithm should consider the amount of load at different buses. A too large discretization unit can lead to a lot of the load shed at some buses to zero. In this paper, we initialize the discretization units for all load buses as 50 MW. In the original cascades for the IEEE 300-bus system, the load shed at 88% of the buses is not less than

TABLE I
NUMBER OF NONZERO ENTRIES IN INTERACTION MATRIX $\boldsymbol{B}$

Matrix	$\boldsymbol{B}^{\mathsf{LL}}$	$\boldsymbol{B}^{\mathsf{BL}}$	$\boldsymbol{B}^{\mathsf{LB}}$	$\boldsymbol{B}^{\mathsf{BB}}$	$\boldsymbol{B}$
Number	1704	36	246	130	2116
Proportion	1.01%	0.05%	0.31%	0.36%	0.58%

25 MW, and thus is discretlized as nonzero integers according to (1). The load shed that is greater than 25 MW accounts for 99.21% of the total amount of load shed.

In Section II the lines and the buses with load are numbered from 1 to N_l and from 1 to N_b, respectively, for convenience. Here, the bus and line index numbers in both the coupled interaction network and the following analysis are those in the original IEEE 300-bus system to avoid confusion.

A. Coupled Interaction Network

We randomly select 10% of the original cascades ($M_{\mathrm{u}} = 3000$) to estimate the coupled interaction matrix $\boldsymbol{B}$. The ε in (16) is set as 0.01. Table I lists the number of nonzero entries in the four sub-matrices of $\boldsymbol{B}$ and the proportion of nonzero entries. The total number of nonzero entries in $\boldsymbol{B}$ is 2,116, which only accounts for 0.58% of the 602^2 entries. Also, $\boldsymbol{B}^{\mathsf{BL}}$ is much sparser than the other sub-matrices, indicating that the chance for load shed to be followed by line outages is very low.

Fig. 2 shows the coupled interaction network of the IEEE 300-bus system. The red and green vertices respectively denote lines and buses with load. The red, blue, yellow, and green arrows are the links in $\boldsymbol{B}^{\mathsf{LL}}$, $\boldsymbol{B}^{\mathsf{LB}}$, $\boldsymbol{B}^{\mathsf{BL}}$, and $\boldsymbol{B}^{\mathsf{BB}}$, respectively. Most links start from red vertices, indicating that line outages are the dominant factors in cascading failure propagation. This is because a more dramatic redistribution of power flow and more heavy-loaded lines tend to be observed after the outages of some critical lines rather than after load shedding at some buses. This is consistent with the conclusion in [22].

The entry b_{iv}^{LB} of the submatrix $\boldsymbol{B}^{\mathsf{LB}}$ captures the interaction that the load shed at bus v follows the outage of line i. The interactions can be further analyzed by the connection of line i and bus v in the transmission system. It is found that bus v is connected with line i only for 9.76% of the 246 interactions in $\boldsymbol{B}^{\mathsf{LB}}$. In addition, in 16.67% of the interactions, line i is connected with generation buses rather than load buses. The result indicates that line outages may not only impact the load supply at the buses that are connected to the outaged line. This can be explained by various complicated causes of the load shed in cascading outages, including but not limited to the isolation of load buses, disconnection of generation buses, and the transmission capacity limits.

B. Validation of Coupled Interaction Model

To test the fit goodness of Poisson distribution with mean b_{iv}^{LB} for the interactions between the outage of line i and the load shed at bus v recorded in $\boldsymbol{C}_{iv}^{\mathsf{LB}}$, the Kolmogorov-Smirnov (K-S) test [36] at the significance level of 0.05 is performed. The results show that the assumption of Poisson distribution is supported by the K-S test for 98.78% of the interactions in $\boldsymbol{B}^{\mathsf{LB}}$ in Table I. Similarly, the K-S test is also performed for the load shed at bus v following the different amounts of discretized load shed at bus u. The results show that the Poisson distribution assumption is supported by the K-S test for all the interactions in $\boldsymbol{B}^{\mathsf{BB}}$ in Table I. This illustrates that the Poisson distribution assumption is valid for the propagation of load shed, which is consistent with [20]–[22].

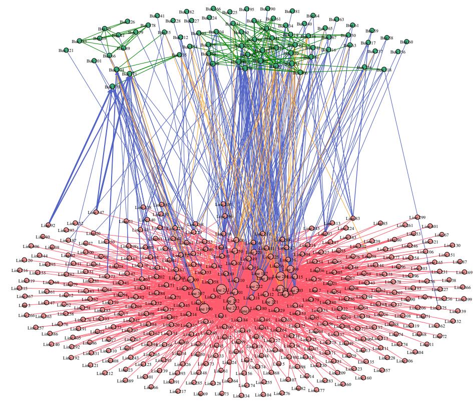

Fig. 2. Coupled interaction network for IEEE 300-bus system.

We simulate 30,000 cascades using the coupled interaction model in Section IV. The distributions of the total number of line outages from 30,000 original cascades and 30,000 simulated cascades are compared in Fig. 3. The distributions of the amount of load shed are compared in Fig. 4. It is seen that the simulated cascades show a consistent distribution of line outages and load shed as the original cascades. Moreover, as seen in Figs. 3 and 4, 3,000 original cascade outages can only estimate blackout size at the probability level of 10^{-3}, while 30,000 simulated cascades from the coupled interaction model can extend the probability level beyond 10^{-4}.

To further validate the impact of the interactions captured by $\boldsymbol{B}^{\mathsf{BL}}$ and $\boldsymbol{B}^{\mathsf{BB}}$, the EM algorithm in Section III and the coupled interaction model in Section IV are modified to only include $\boldsymbol{B}^{\mathsf{LL}}$ and $\boldsymbol{B}^{\mathsf{LB}}$. The modified interaction model is referred to as the reduced interaction model. Figs. 3 and 4 compare the probability distributions of the outages from the interaction model and the reduced interaction model. Fig. 3 shows that $\boldsymbol{B}^{\mathsf{BL}}$ has a marginal impact on the propagation of line outages. This is because the number of nonzero elements in $\boldsymbol{B}^{\mathsf{BL}}$ is much smaller than that in $\boldsymbol{B}^{\mathsf{LL}}$. However, it is found from Fig. 4 that $\boldsymbol{B}^{\mathsf{BB}}$ has a noticeable impact on the propagation of load shed, especially on large load shed. This is due to the fact that large blackouts often involve successive load shedding, which is effectively captured by $\boldsymbol{B}^{\mathsf{BB}}$.

As only 10% of original cascades are used to estimate the interaction matrix $\boldsymbol{B}$, the highly probabilistic interaction model can significantly improve the simulation efficiency. Simulating 30,000 cascades by OPA model takes 9,214 seconds, while the simulation with the coupled interaction model takes only 47 seconds. The time required to generate 3,000 original cascades is $3000/30000 \times 9214 \approx 921$ seconds, and the time for the EM algorithm is 52 seconds. Therefore, a speed-up of $9214/(921+52+47) \approx 9.03$ can be achieved by the coupled interaction model for simulating 30,000 cascades.

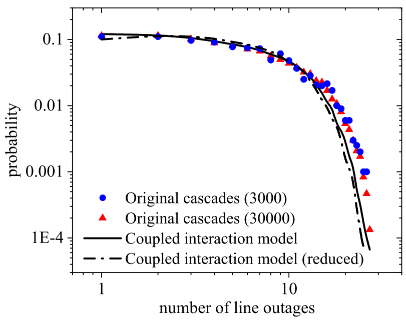

Fig. 3. Probability distribution of the total number of line outages.

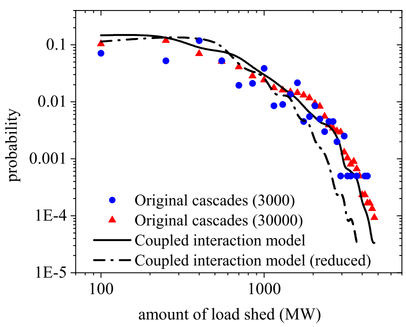

Fig. 4. Probability distribution of the total amount of load shed.

C. Choosing Critical Links for Mitigation

To mitigation the propagation of cascading failure through link $l : S \to T$, remedial actions can be implemented to reduce the probability of outage T when source outage S occurs. Table II lists the top 5 of each type of links ranked according to I_l in (33) with $c^{\mathrm{L}} = 1$ and $c^{\mathrm{B}} = 1.5$.

The target outage T in $\mathsf{L} \to \mathsf{B}$ and $\mathsf{B} \to \mathsf{B}$ links is load shed at a bus. As the location and amount of load shed in cascading outages are determined manually by the operators or automatically by the relays, the priority of the buses in $\mathsf{L} \to \mathsf{B}$ and $\mathsf{B} \to \mathsf{B}$ links for load shed can be adjusted with respect to the source outages. For the manual load shed, the priority of the bus in target outages can be adjusted by increasing its load shed cost in the optimal power flow problem. For the automatic load shed, the adaptive load shedding [37], which is supported by the wide-area monitoring system, adjusts the priority of buses online with respect to the disturbances.

In this paper, to mitigate the load shed as the target outage T, the load shed cost of outage T is increased in the optimal power flow problem in OPA model. After increasing the load shed cost by ten times for the critical $\mathsf{L} \to \mathsf{B}$ and $\mathsf{B} \to \mathsf{B}$ links in Table II, an average reduction of 4.4% of the number of times of outage T and 6.1% of the amount of load shed is observed. The load shed of outage T is not reduced effectively, mainly because in cascading failure models such as OPA the load shed is mainly caused by generation shortage in islands or insufficient transmission capacity following the outage of critical lines, and the increase of load shed cost cannot avoid the occurrence of most load shedding. As the load shed cannot be effectively mitigated by directly reducing its probability after the occurrence of source outage S, another way to indirectly mitigate load shedding is to reduce the probability of line outages as the source outages in critical $\mathsf{L} \to \mathsf{B}$ links.

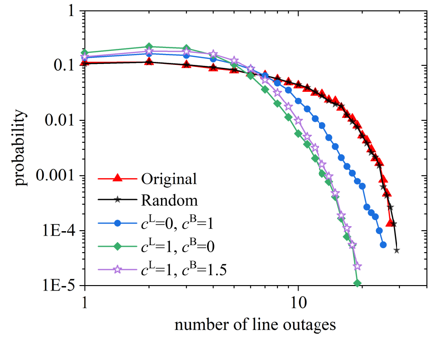

Fig. 5. Probability distribution of the number of line outage under different mitigation strategies.

On the other hand, the target outage T in $\mathsf{L} \to \mathsf{L}$ and $\mathsf{B} \to \mathsf{L}$ links is a line outage. To mitigate line outages as the target outage T, the probability of outage T can be reduced by blocking the Zone 3 relay [24] or increasing the transfer margin of the targeted line [38]. It is seen in Table II that the indices of $\mathsf{B} \to \mathsf{L}$ links are much smaller than those of $\mathsf{L} \to \mathsf{L}$ links. Moreover, critical $\mathsf{B} \to \mathsf{L}$ links tend to have $\mathsf{L} \to \mathsf{L} \to \mathsf{B}$ link chains pointing to them. Take the link "bus 204 $\to$ line 309" as an example, which is the top one $\mathsf{B} \to \mathsf{L}$ link in Table II. The link chain "line 268 $\to$ line 307 $\to$ bus 204" points to "bus 204 $\to$ line 309". Mitigating the critical link "line 268 $\to$ line 307" reduces the probability of load shedding at bus 204 and further line 309 outage. In addition, as line 309 outage is likely to follow both the critical link "line 268 $\to$ line 309" and the link chain "line 268 $\to$ bus 204 $\to$ line 309", reducing the probability of line 309 outage by the $\mathsf{B} \to \mathsf{L}$ link "bus 204 $\to$ line 309" can be covered by the $\mathsf{L} \to \mathsf{L}$ link.

Based on the above analysis it is practical to mitigate the propagation of cascading failures by only considering the critical $\mathsf{L} \to \mathsf{L}$ links. In Section VI-D we will only consider critical $\mathsf{L} \to \mathsf{L}$ links based mitigation.

D. Cascading Failure Mitigation

Here mitigation strategy is implemented based on the identified $\mathsf{L} \to \mathsf{L}$ critical links by blocking Zone 3 relay [24]. For example, for critical link $l : \mathrm{line}\, i \to \mathrm{line}\, j$, when line i fails, the relay of line j is blocked to reduce its tripping probability to 10% of its original probability so that the control center could perform remedy control and stop failure propagation.

The following four mitigation strategies are implemented.

1) Relay blocking is based on 30 randomly selected links.
2) Relay blocking is based on top 30 links ranked by I_l with $c^{\mathsf{L}} = 0$ and $c^{\mathsf{B}} = 1$.
3) Relay blocking is based on top 30 links ranked by I_l with $c^{\mathsf{L}} = 1$ and $c^{\mathsf{B}} = 0$.
4) Relay blocking is based on top 30 links ranked by I_l with $c^{\mathsf{L}} = 1$ and $c^{\mathsf{B}} = 1.5$.

For each mitigation strategy, 150,000 cascades are generated by the OPA model with relay blocking for the corresponding links [24]. In this paper, when the source outage S happens

TABLE II
TOP 5 CRITICAL LINKS RANKED ACCORDING TO I_l WHEN $c^{\mathsf{L}} = 1$ AND $c^{\mathsf{B}} = 1.5$

L → L link	I_l	L → B link	I_l	B → L link	I_l	B → B link	I_l
line 268 → line 309	2.35	line 307 → bus 171	7.93	bus 204 → line 309	0.32	bus 120 → bus 100	0.19
line 251 → line 252	1.96	line 309 → bus 171	6.97	bus 152 → line 249	0.23	bus 106 → bus 106	0.16
line 223 → line 222	1.89	line 268 → bus 171	5.67	bus 99 → line 178	0.21	bus 106 → bus 163	0.12
line 309 → line 268	1.44	line 268 → bus 204	5.62	bus 170 → line 268	0.19	bus 146 → bus 146	0.12
line 268 → line 307	1.31	line 307 → bus 204	4.74	bus 152 → line 247	0.15	bus 138 → bus 120	0.10

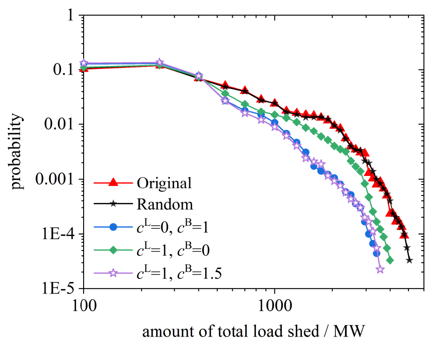

Fig. 6. Probability distribution of the amount of load shed under different mitigation strategies.

in generation g of cascade m, the relay is blocked for the target outage T in all remaining generations of cascade m. Figs. 5 and 6 compare the probability distributions of the number of line outages and the amount of load shed before and after mitigation. As in Fig. 5, the number of line outages is mitigated the most by the third mitigation strategy since only line outage consequence is considered ($c^{\mathsf{B}} = 0$). However, the reduction of load shed is not as effective as the strategies that consider load shed consequences. Similarly, as in Fig. 6, when the second strategy only considers the cost of load shed ($c^{\mathsf{L}} = 0$), the amount of load shed is mitigated the most but the line outage is not mitigated very well. By properly setting $c^{\mathsf{L}}/c^{\mathsf{B}} = 1/1.5$, the fourth mitigation strategy is able to make a tradeoff and reduce both line outage and load shed to a great extent, leading to the best mitigation effect in terms of both line outage and load shed consequences.

To evaluate the mitigation effect, the size of cascades is classified into small, medium, and large cascade in terms of the total number of line outages (τ^{L}), the total amount of load shed (τ^{B}), or a comprehensive cost (τ). The comprehensive cost τ is calculated by assuming that the ratio between the cost of the normalized line outage and that of the normalized load shed is $1/1.5$ as:

$$\tau = \frac{\tau^{\mathsf{L}}}{N_l} + 1.5\frac{\tau^{\mathsf{B}}}{X^{\mathrm{t}}}. \tag{34}$$

Tables III–V compare the probabilities of small, medium, and large cascades under the four mitigation strategies. Note that the samples in Tables III–V for large cascades are no less than 11 in order to estimate the probabilities of large cascades with a confidence level of 95% [39]. As in Tables III–IV, when $c^{\mathsf{L}} = 1$ and $c^{\mathsf{B}} = 1.5$ the mitigation effect in terms of line outage is similar to the case in which $c^{\mathsf{L}} = 1$ and $c^{\mathsf{B}} = 0$

TABLE III
PROBABILITIES OF DIFFERENT CASCADE SIZES MEASURED BY τ^{L}

Cases	small $\tau^{\mathsf{L}} \le 15$	medium $15 < \tau^{\mathsf{L}} \le 25$	large $\tau^{\mathsf{L}} > 25$
No mitigation	0.8872	0.1095	0.0033
Random	0.8932	0.1040	0.0028
c^{L}=0, c^{B}=1	0.9856	0.0142	1.53×10^{-4}
c^{L}=1, c^{B}=0	0.9985	0.0015	0
c^{L}=1, c^{B}=1.5	0.9982	0.0018	0

TABLE IV
PROBABILITIES OF DIFFERENT CASCADE SIZES MEASURED BY τ^{B}

Cases	small $\tau^{\mathsf{B}} \le 1500$	medium $1500 < \tau^{\mathsf{B}} \le 3000$	large $\tau^{\mathsf{B}} > 3000$
No mitigation	0.9129	0.0798	0.0073
Random	0.9144	0.0781	0.0075
c^{L}=0, c^{B}=1	0.9916	0.0082	2.13×10^{-4}
c^{L}=1, c^{B}=0	0.9584	0.0405	0.0011
c^{L}=1, c^{B}=1.5	0.9910	0.0087	3.34×10^{-4}

TABLE V
PROBABILITIES OF DIFFERENT CASCADE SIZES MEASURED BY τ

Cases	small $\tau \le 0.15$	medium $0.15 < \tau \le 0.30$	large $\tau > 0.30$
No mitigation	0.9483	0.0506	0.0011
Random	0.9485	0.0502	0.0013
c^{L}=0, c^{B}=1	0.9963	0.0037	0
c^{L}=1, c^{B}=0	0.9901	0.0098	8.67×10^{-5}
c^{L}=1, c^{B}=1.5	0.9971	0.0029	0

while the mitigation effect in terms of load shed is similar to the case in which $c^{\mathsf{L}} = 0$ and $c^{\mathsf{B}} = 1$. It is seen from Table V that a proper choice of c^{L} and c^{B} enables the fourth strategy to provide the most reduction of the medium and large cascades in terms of the comprehensive cost.

Finally, to validate the optimality of the fourth strategy, a greedy algorithm in [40] is also used to identify the critical links from the coupled interaction network. The optimal blocked links are chosen in [40] to minimize the spread of contamination in the independent cascade (IC) model, a high-level statistical model similar to the proposed coupled interaction model. The details of the greedy algorithm can be found in [40]. Here only the specific definitions for cascading outages are introduced. Firstly, the sampling of graph in [40] can be done by simulating cascades using the coupled interaction model. To be specific, when an outage is generated for a line or a bus in the simulation, the corresponding node in the coupled interaction network is activated. And when an outage generates another new outage, the corresponding

TABLE VI
COMPARISON OF TOP 10 CRITICAL LINKS WITH RESPECT TO I_l AND THE GREEDY ALGORITHM

Critical links	Rank	
	I_l	Greedy
line 268 → line 309	1	1
line 251 → line 252	2	2
line 223 → line 222	3	3
line 309 → line 268	4	4
line 268 → line 307	5	6
line 190 → line 197	6	7
line 190 → line 199	7	9
line 250 → line 249	8	11
line 222 → line 225	9	12
line 190 → line 204	10	5

propagation link is activated. All the activated nodes and links in a cascade compose a directed graph. In cascade m, outage j is reachable from outage i if there is a path from i to j along the activated links. The reachable node set for outage i in cascade m is calculated as $\tau(i,m)$ below:

$$\tau(i,m)=\frac{\tau^{\mathsf{L}}(i,m)}{N_l}+1.5\frac{\tau^{\mathsf{B}}(i,m)}{X^{\mathrm{t}}}, \tag{35}$$

where $\tau^{\mathsf{L}}(i,m)$ is the total number of line outages reachable from line i in cascade m, and $\tau^{\mathsf{B}}(i,m)$ is the total amount of load shed at the buses reachable from line i in cascade m.

With the above definitions, the greedy algorithm in [40] can be applied to choose critical $\mathsf{L}\rightarrow\mathsf{L}$ links from the coupled interaction network by calculating the average reachable node set for activated nodes in the sampled graphs. In this paper, each $\mathsf{L}\rightarrow\mathsf{L}$ link is chosen with 30,000 cascades simulated by the coupled interaction model. After the choice of one $\mathsf{L}\rightarrow\mathsf{L}$ link, the corresponding entry b_{ij}^{LL} of $\boldsymbol{B}^{\mathsf{LL}}$ is set to be zero to mimic the removal of the link from the network in [40]. And the next blocked link is chosen using another 30,000 cascades simulated with the updated interaction matrix. Namely, 30×30,000 cascades are simulated in total to choose the top 30 links.

The result shows that 27 out of 30 critical links in the greedy algorithm are also chosen as critical links by the fourth strategy. The remaining 3 links rank, respectively, 33rd, 36th and 38th with respect to I_l. Table VI compares the top 10 critical links chosen by using I_l and the greedy algorithm. It is seen that the fourth strategy and the greedy algorithm identify similar critical links. Figs. 7 and 8 compare the mitigation effects of the fourth strategy and the greedy algorithm, which are very close due to the similarity of critical links.

VII. CONCLUSION

In this paper, a coupled interaction matrix is proposed and estimated by EM algorithm in order to extract useful information about cascading propagation of interdependent line outages and the load shed. A highly probabilistic interaction model is further proposed based on the coupled interaction matrix to enable efficient cascading failure simulation. Based on the coupled interaction matrix, critical links are identified by calculating a comprehensive severity index that considers the consequences of both line outages and the load shed.

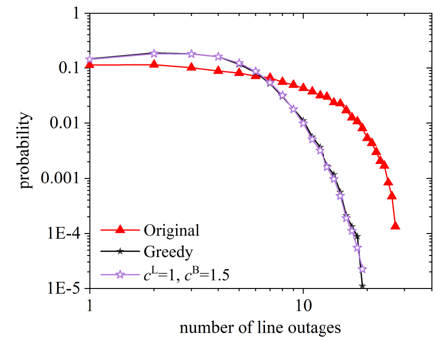

Fig. 7. Probability distribution of the number of line outages under the fourth strategy and the greedy algorithm.

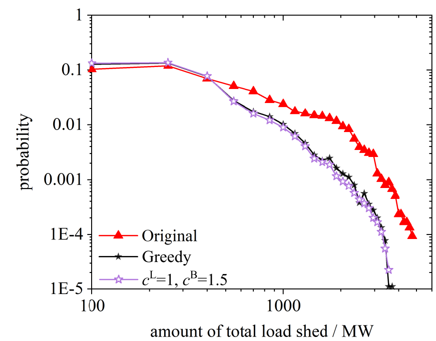

Fig. 8. Probability distribution of the amount of load shed under the fourth strategy and the greedy algorithm.

Simulation results on the IEEE 300-bus system validate the effectiveness of the proposed coupled interaction model in capturing the statistical properties of the original cascades and demonstrate that a speed-up of 9.03 is achieved when simulating 30,000 cascades. It is also found that the links between line outages are dominant factors in the propagation of cascading failures. Besides, the identified critical links based on the proposed comprehensive severity index enable a proper tradeoff between reducing line outages and reducing the load shed, leading to a better mitigation effect than only considering either line outages or the load shed.

In addition to line outages and the load shed, other types of events can also be incorporated into the coupled interaction model. For example, similar to [22], the number of isolated buses can also be analyzed together with line outages and the load shed. The tripping events of generators reported in recent blackouts [41], which may be caused following the voltage disturbances after line faults, also deserve attention. The coupled interaction model is promising for capturing the propagation of isolated buses or the generator outages, which are discrete events similar to line outages in blackouts. The interactions among line outages, load shed, and isolated buses/generator outages will be investigated in the future.

APPENDIX

The choice of the discretization unit for each load bus is discussed as follows. Let $\tilde{\lambda}_{iv}^{(k+1)}$ and $\tilde{\sigma}_{iv}^{2(k+1)}$ be the mean and the variance of the discretized load shed at bus v following the outage of line i when $\Delta_v^{(k)}$ is chosen as the discretization unit for bus v. If we change the discretization unit for bus v to $\Delta_v^{(k+1)}$, the mean changes to $\lambda_{iv}^{(k+1)} = \tilde{\lambda}_{iv}^{(k+1)}\Delta_v^{(k)}/\Delta_v^{(k+1)}$, and the variance changes to $\sigma_{iv}^{2(k+1)} = \tilde{\sigma}_{iv}^{2(k)}\left(\Delta_v^{(k)}\right)^2/\left(\Delta_v^{(k+1)}\right)^2$. Note that the mean of the Poisson distribution equals its variance. A better choice of $\Delta_v^{(k+1)}$ should make the mean $\lambda_{iv}^{(k+1)}$ close to the variance $\sigma_{iv}^{2(k+1)}$ as much as possible. Moreover, the choice of $\Delta_v^{(k+1)}$ should consider all the lines whose outages have interactions with the load shed at bus v. Thus, to choose the optimal discretization unit $\Delta_v^{(k+1)}$ for bus v, the following optimization problem (36) can be solved:

$$\min\ f\left(\Delta_v^{(k+1)}\right) = \sum_{i\in\mathcal{S}_v^{\mathsf{LB}}} N_i^{\mathsf{L}}\left(\frac{\lambda_{iv}^{(k+1)}}{\sigma_{iv}^{2(k+1)}} + \frac{\sigma_{iv}^{2(k+1)}}{\lambda_{iv}^{(k+1)}}\right) \quad (36)$$

$$\text{s.t.}\quad \lambda_{iv}^{(k+1)} = \frac{\Delta_v^{(k)}}{\Delta_v^{(k+1)}}\tilde{\lambda}_{iv}^{(k+1)} \quad (37)$$

$$\sigma_{iv}^{2(k+1)} = \left(\frac{\Delta_v^{(k)}}{\Delta_v^{(k+1)}}\right)^2\tilde{\sigma}_{iv}^{2(k+1)}. \quad (38)$$

It is easy to obtain the optimal solution as

$$\Delta_v^{(k+1)} = \Delta_v^{(k)}\sqrt{\frac{\sum\limits_{i\in\mathcal{S}_v^{\mathsf{LB}}} N_i^{\mathsf{L}}\frac{\tilde{\sigma}_{iv}^{2(k+1)}}{\tilde{\lambda}_{iv}^{(k+1)}}}{\sum\limits_{i\in\mathcal{S}_v^{\mathsf{LB}}} N_i^{\mathsf{L}}\frac{\tilde{\lambda}_{iv}^{(k+1)}}{\tilde{\sigma}_{iv}^{2(k+1)}}}}. \quad (39)$$

If we consider $\tilde{\lambda}_{iv}^{(k+1)} \approx \tilde{b}_{iv}^{\mathsf{LB}(k+1)}$ and $\tilde{\sigma}_{iv}^{2(k+1)} \approx S_{iv}^{2(k+1)}$, then $\Delta_v^{(k+1)}$ can be chosen as

$$\Delta_v^{(k+1)} = \Delta_v^{(k)}\sqrt{\frac{\sum\limits_{i\in\mathcal{S}_v^{\mathsf{LB}}} N_i^{\mathsf{L}}\frac{S_{iv}^{2(k+1)}}{\tilde{b}_{iv}^{\mathsf{LB}(k+1)}}}{\sum\limits_{i\in\mathcal{S}_v^{\mathsf{LB}}} N_i^{\mathsf{L}}\frac{\tilde{b}_{iv}^{\mathsf{LB}(k+1)}}{S_{iv}^{2(k+1)}}}}.$$

ACKNOWLEDGMENT

The authors would like to thank Dr. Wenyun Ju for his valuable discussions regarding cascading failure mitigation.

REFERENCES

[1] K. Sun, Y. Hou, W. Sun, and J. Qi, *Power System Control under Cascading Failures: Understanding, Mitigation, and Restoration*. Wiley-IEEE Press, Jan. 2019.
[2] Y. Yang, T. Nishikawa, and A. E. Motter, "Small vulnerable sets determine large network cascades in power grids," *Science*, vol. 358, no. 6365, 2017.
[3] I. Dobson, B. Carreras, V. Lynch, and D. Newman, "An initial model for complex dynamics in electric power system blackouts," in *Proc. 34th Hawaii Int. Conf. System Sciences*, 2001, pp. 710–718.
[4] S. Mei, F. He, X. Zhang, S. Wu, and G. Wang, "An improved OPA model and blackout risk assessment," *IEEE Trans. Power Syst.*, vol. 24, no. 2, pp. 814–823, May 2009.
[5] J. Qi, S. Mei, and F. Liu, "Blackout model considering slow process," *IEEE Trans. Power Syst.*, vol. 28, no. 3, pp. 3274–3282, Jan. 2013.
[6] M. A. Rios, D. S. Kirschen, D. Jayaweera, D. P. Nedic, and R. N. Allan, "Value of security: modeling time-dependent phenomena and weather conditions," *IEEE Trans. Power Syst.*, vol. 17, no. 3, pp. 543–548, Aug. 2002.
[7] J. Song, E. Cotilla-Sanchez, G. Ghanavati, and P. D. H. Hines, "Dynamic modeling of cascading failure in power systems," *IEEE Trans. Power Syst.*, vol. 31, no. 3, pp. 2085–2095, May 2016.
[8] R. Yao, S. Huang, K. Sun, F. Liu, X. Zhang, and S. Mei, "A multi-timescale quasi-dynamic model for simulation of cascading outages," *IEEE Trans. Power Syst.*, vol. 31, no. 4, pp. 3189–3201, Jul. 2016.
[9] I. Dobson, A. Flueck, S. Aquiles-Perez, S. Abhyankar, and J. Qi, "Towards incorporating protection and uncertainty into cascading failure simulation and analysis," in *IEEE Int. Conf. Probabilistic Methods Applied to Power Systems (PMAPS)*, Jun. 2018, pp. 1–5.
[10] S. R. Khazeiynasab and J. Qi, "Resilience analysis and cascading failure modeling of power systems under extreme temperatures," *Journal of Modern Power Systems and Clean Energy*, 2020.
[11] J. Bialek *et al.*, "Benchmarking and validation of cascading failure analysis tools," *IEEE Trans. Power Syst.*, vol. 31, no. 6, pp. 4887–4900, 2016.
[12] P. Rezaei, P. D. H. Hines, and M. J. Eppstein, "Estimating cascading failure risk with random chemistry," *IEEE Trans. Power Syst.*, vol. 30, no. 5, pp. 2726–2735, Sept. 2015.
[13] J. Guo, F. Liu, J. Wang, J. Lin, and S. Mei, "Toward efficient cascading outage simulation and probability analysis in power systems," *IEEE Trans. Power Syst.*, vol. 33, no. 3, pp. 2370–2382, May 2018.
[14] Y. Liu, Y. Wang, P. Yong, N. Zhang, C. Kang, and D. Lu, "Fast power system cascading failure path searching with high wind power penetration," *IEEE Trans. Sustain. Energy*, vol. 11, no. 4, pp. 2274–2283, Oct. 2020.
[15] P. Dey, R. Mehra, F. Kazi, S. Wagh, and N. M. Singh, "Impact of topology on the propagation of cascading failure in power grid," *IEEE Trans. Smart Grid*, vol. 7, no. 4, pp. 1970–1978, Jul. 2016.
[16] J. Beyza, E. Garcia-Paricio, H. F. Ruiz, and J. M. Yusta, "Geodesic vulnerability approach for identification of critical buses in power systems," *J. Mod. Power Syst. Clean Energy*, Early Access, DOI: 10.35833/MPCE.2018.000779.
[17] K.-I. Goh, D.-S. Lee, B. Kahng, and D. Kim, "Sandpile on scale-free networks," *Physical review letters*, vol. 91, no. 14, p. 148701, Oct. 2003.
[18] J. Qi and S. Pfenninger, "Controlling the self-organizing dynamics in a sandpile model on complex networks by failure tolerance," *EPL (Europhysics Letters)*, vol. 111, no. 3, p. 38006, Aug. 2015.
[19] I. Dobson, "Estimating the propagation and extent of cascading line outages from utility data with a branching process," *IEEE Trans. Power Syst.*, vol. 27, no. 4, pp. 2146–2155, Nov. 2012.
[20] J. Kim, K. R. Wierzbicki, I. Dobson, and R. C. Hardiman, "Estimating propagation and distribution of load shed in simulations of cascading blackouts," *IEEE Syst. J.*, vol. 6, no. 3, pp. 548–557, Sept. 2012.
[21] J. Qi, I. Dobson, and S. Mei, "Towards estimating the statistics of simulated cascades of outages with branching processes," *IEEE Trans. Power Syst.*, vol. 28, no. 3, pp. 3410–3419, Aug. 2013.
[22] J. Qi, W. Ju, and K. Sun, "Estimating the propagation of interdependent cascading outages with multi-type branching processes," *IEEE Trans. Power Syst.*, vol. 32, no. 2, pp. 1212–1223, Mar. 2017.
[23] I. Dobson, B. A. Carreras, and D. E. Newman, "A branching process approximation to cascading load-dependent system failure," in *Proc. 37th Hawaii Int. Conf. System Sciences*, 2004, pp. 1–10.
[24] J. Qi, K. Sun, and S. Mei, "An interaction model for simulation and mitigation of cascading failures," *IEEE Trans. Power Syst.*, vol. 30, no. 2, pp. 804–819, March. 2015.
[25] J. Qi, J. Wang, and K. Sun, "Efficient estimation of component interactions for cascading failure analysis by EM algorithm," *IEEE Trans. Power Syst.*, vol. 33, no. 3, pp. 3153–3161, May 2018.
[26] W. Ju, K. Sun, and J. Qi, "Multi-layer interaction graph for analysis and mitigation of cascading outages," *IEEE J. Emerg. Sel. Top. Circuits Syst.*, vol. 7, no. 2, pp. 239–249, Jun. 2017.
[27] J. Qi, "Utility outage data driven interaction networks for cascading failure analysis and mitigation," *IEEE Trans. Power Syst.*, 2020, Early Access.
[28] P. D. Hines, I. Dobson, E. Cotilla-Sanchez, and M. Eppstein, ""dual graph" and "random chemistry" methods for cascading failure analysis," in *Proc. 46th Hawaii Int. Conf. System Sciences*, 2013, pp. 2141–2150.
[29] P. D. H. Hines, I. Dobson, and P. Rezaei, "Cascading power outages propagate locally in an influence graph that is not the actual grid topology," *IEEE Trans. Power Syst.*, vol. 32, no. 2, pp. 958–967, March. 2017.
[30] K. Zhou, I. Dobson, Z. Wang, A. Roitershtein, and A. P. Ghosh, "A markovian influence graph formed from utility line outage data to mitigate large cascades," *IEEE Trans. Power Syst.*, vol. 35, no. 4, pp. 3224–3235, July 2020.
[31] A. Shandilya, H. Gupta, and J. Sharma, "Method for generation rescheduling and load shedding to alleviate line overloads using local optimisation," *IEE Proc. C Gener. Transm. Distrib.*, vol. 140, no. 5, pp. 337–342, Sept. 1993.

[32] D. Novosel and R. L. King, "Using artificial neural networks for load shedding to alleviate overloaded lines," *IEEE Trans. Power Deliv.*, vol. 9, no. 1, pp. 425–433, Jan 1994.
[33] K. Saito, R. Nakano, and M. Kimura, "Prediction of information diffusion probabilities for independent cascade model," in *KES*. Springer, 2008, pp. 67–75.
[34] M. Vaiman, K. Bell, Y. Chen, B. Chowdhury, I. Dobson, P. Hines, M. Papic, S. Miller, and P. Zhang, "Risk assessment of cascading outages: Methodologies and challenges," *IEEE Trans. Power Syst.*, vol. 27, no. 2, p. 631, May 2012.
[35] Power Systems Test Case Archive. Univ.Washington. [Online]. Available: http://www.ee.washington.edu/research/pstca/.
[36] F. J. Massey Jr, "The Kolmogorov-Smirnov test for goodness of fit," *J. Am. Stat. Assoc.*, vol. 46, no. 253, pp. 68–78, 1951.
[37] H. H. Alhelou, M. E. H. Golshan, T. C. Njenda, and N. D. Hatziargyriou, "An overview of UFLS in conventional, modern, and future smart power systems: Challenges and opportunities," *Electr. Power Syst. Res.*, vol. 179, p. 106054, Feb. 2020.
[38] C. Chen, W. Ju, K. Sun, and S. Ma, "Mitigation of cascading outages using a dynamic interaction graph-based optimal power flow model," *IEEE Access*, vol. 7, pp. 168 637–168 648, 2019.
[39] I. Dobson, B. A. Carreras, and D. E. Newman, "How many occurrences of rare blackout events are needed to estimate event probability?" *IEEE Trans. Power Syst.*, vol. 28, no. 3, pp. 3509–3510, Aug. 2013.
[40] M. Kimura, K. Saito, and H. Motoda, "Minimizing the spread of contamination by blocking links in a network." in *AAAI*, vol. 8, 2008, pp. 1175–1180.
[41] Australian Energy Market Operator (AEMO). (2017, Mar.). Black System South Australia 28 September 2016. [Online]. Available: https://www.aemo.com.au

Leibao Wang received the B.E. degree from the School of Electrical Engineering, Xi'an Jiaotong University, Xi'an, China, in 2016. He is currently pursuing the Ph.D. degree in the School of Electrical Engineering, Chongqing University, Chongqing, China. He was a Visiting Scholar with Stevens Institute of Technology, Hoboken, NJ, USA, in 2020. His major research interests include power system reliability and cascading failures.

Junjian Qi (S'12–M'13–SM'17) received the B.E. degree in electrical engineering, from Shandong University, Jinan, China, in 2008, and the Ph.D. degree in electrical engineering from Tsinghua University, Beijing, China, in 2013. He was a Visiting Scholar with Iowa State University, Ames, IA, USA, in 2012, a Research Associate with the Department of EECS, University of Tennessee, Knoxville, TN, USA, from 2013 to 2015, a Postdoctoral Appointee with the Energy Systems Division, Argonne National Laboratory, Lemont, IL, USA, from 2015 to 2017, and an Assistant Professor with the Department of Electrical and Computer Engineering, University of Central Florida, Orlando, FL, USA, from 2017 to 2020. He is currently an Assistant Professor with the Department of Electrical and Computer Engineering, Stevens Institute of Technology, Hoboken, NJ, USA. He was the recipient of the NSF CAREER award in 2020 and is an Associate Editor for the IEEE Access. His research interests include cascading blackouts, microgrid control, cyber-physical systems, and synchrophasors.

Bo Hu (M'14) was born in Henan, China, in 1983. He received the Ph.D. degree in electrical engineering from Chongqing University, Chongqing, China, in 2010, where he is currently a Professor with the School of Electrical Engineering. His research interests include power system reliability and parallel computing techniques in power systems.

Kaigui Xie (M'10–SM'13) received the Ph.D. degree in power system and its automation from Chongqing University, Chongqing, China, in 2001. He is currently a Full Professor with the School of Electrical Engineering, Chongqing University. He has authored and coauthored over 200 academic articles and six books. His main research interests include power system reliability, planning, and analysis. He is a Fellow of IET. He was awarded the title of the National Science Fund for Outstanding Young Scholar. He is an Editor of the IEEE Transactions on Power Systems and an Associate Editor of IET Proceedings-Generation, Transmission and Distribution.